Laser Magnetic Resonance

Al Chichinin, Institute of Chemical Kinetics and Combustion, Novosibirsk, Russia

MAGNETIC RESONANCE
Methods & Instrumentation

Laser magnetic resonance (LMR) is a sensitive technique for studying rotational, vibrational-rotational, or electronic Zeeman spectra of paramagnetic atoms and molecules, using fixed-frequency infrared lasers. High resolution and sensitivity are important characteristics of LMR. In a pioneering experiment in 1968, Evenson and his coworkers succeeded in demonstrating the feasibility of this technique when they detected a rotational transition of O_2 using a HCN laser. Several years later LMR was extended to the mid-infrared by using CO and CO_2 lasers with similar success. Since then, throughout 15 years, much of the increase in understanding of the structure and properties of short-lived paramagnetic molecules has come from the application of LMR. The method has allowed the detection of more than 100 free radicals, including elusive species such as HO_2, CH_2, FO and $Cl(^2P_{1/2})$ which cannot easily be detected by other means. The high sensitivity and versatility of LMR has resulted in numerous applications of the method to chemical kinetics.

Theory of LMR

Atoms

As a simple illustration let us consider the LMR spectra of Cl atoms. The energy level diagram at the top of **Figure 1** shows the Zeeman effect in Cl atoms.

In a magnetic field, the $|J, I, F\rangle$ levels of the atom split into components labelled by M_J and M_F quantum numbers (here $\boldsymbol{F} = \boldsymbol{J} + \boldsymbol{I} = \boldsymbol{L} + \boldsymbol{S} + \boldsymbol{I}$). The magnetic field is swept, and at suitable values of the field the frequencies of the transitions $|J, M_J, M_F\rangle \rightarrow \langle J', M'_J, M'_F|$ come into coincidence with the frequency of a fixed-frequency laser. These resonances result in a decrease in detected laser power. In practice, a small modulation (up to 50 G) is added to the magnetic field and the change in transmitted laser power is recorded as a first derivative signal by processing the detector output in a phase-sensitive amplifier.

LMR spectra of Cl atoms are shown at the bottom of **Figure 1**. Note that $^2P_{3/2}$–$^2P_{1/2}$ magnetic dipole transitions with $\Delta M_F = \pm 1$ and $\Delta M_F = 0$ occur at $\boldsymbol{E} \perp \boldsymbol{B}$ and $\boldsymbol{E} \parallel \boldsymbol{B}$ polarizations, respectively; here $\boldsymbol{E}$ is the electric field of the laser radiation and $\boldsymbol{B}$ is the magnetic field of the electromagnet.

The Hamiltonian may be written as

$$H = A_{so}\boldsymbol{LS} + H_{hfs}(a, b, \boldsymbol{J}, \boldsymbol{I}) + \mu_0(g_J\boldsymbol{JB} + g_I\boldsymbol{IB})$$

where H_{hfs} is the hyperfine interaction operator, A_{so} is a spin-orbit interaction constant, a and b are hyperfine constants, $\mu_0 = e\hbar/2mc$ is the Bohr magneton, and g_J and g_I are electron and nuclear g-factors. All these atomic constants can be obtained from the analysis of LMR spectra; the precise values for A_{so} have been determined in this way for the first time.

Diatomic radicals

A more common application is the measurement of LMR spectra of linear radicals with both spin and orbital angular momentum (SnH, NiH, GeH, CH, SD, SeH, ... etc). The effective Hamiltonian is a summation of spin-orbit (H_{so}), vibrational (H_v), rotational (H_{rot}), spin-rotational (H_{sr}), spin-spin (H_{ss}), lambda-doubling (H_{ld}), hyperfine (H_{hfs}) and Zeeman (H_z) terms:

$$H = H_{so} + H_v + H_{rot} + H_{sr} + H_{ss} + H_{ld} + H_{hfs} + H_z \qquad [1]$$

The choice of significant terms and representation of the terms are determined by the particular type of radical. Some usual representations are presented below

$$H_{so} = A_{so}\,\boldsymbol{LS}$$
$$H_v = \hbar\omega_e(v + 1/2) - \omega_e x_e \hbar(v + 1/2)^2$$
$$H_{rot} = B_v\boldsymbol{N}^2 - D_v\boldsymbol{N}^4$$
$$H_{sr} = \gamma\boldsymbol{NS}$$
$$H_{ss} = \frac{2}{3}\lambda(3S_z^2 - \boldsymbol{S}^2)$$
$$H_z = \mu_0(g_s\boldsymbol{S} + g_L\boldsymbol{L} + g_r\boldsymbol{N})\boldsymbol{B}$$

Here v denotes the vibrational quantum number and $\boldsymbol{N} = \boldsymbol{J} - \boldsymbol{L} - \boldsymbol{S}$ is the nuclear rotational angular

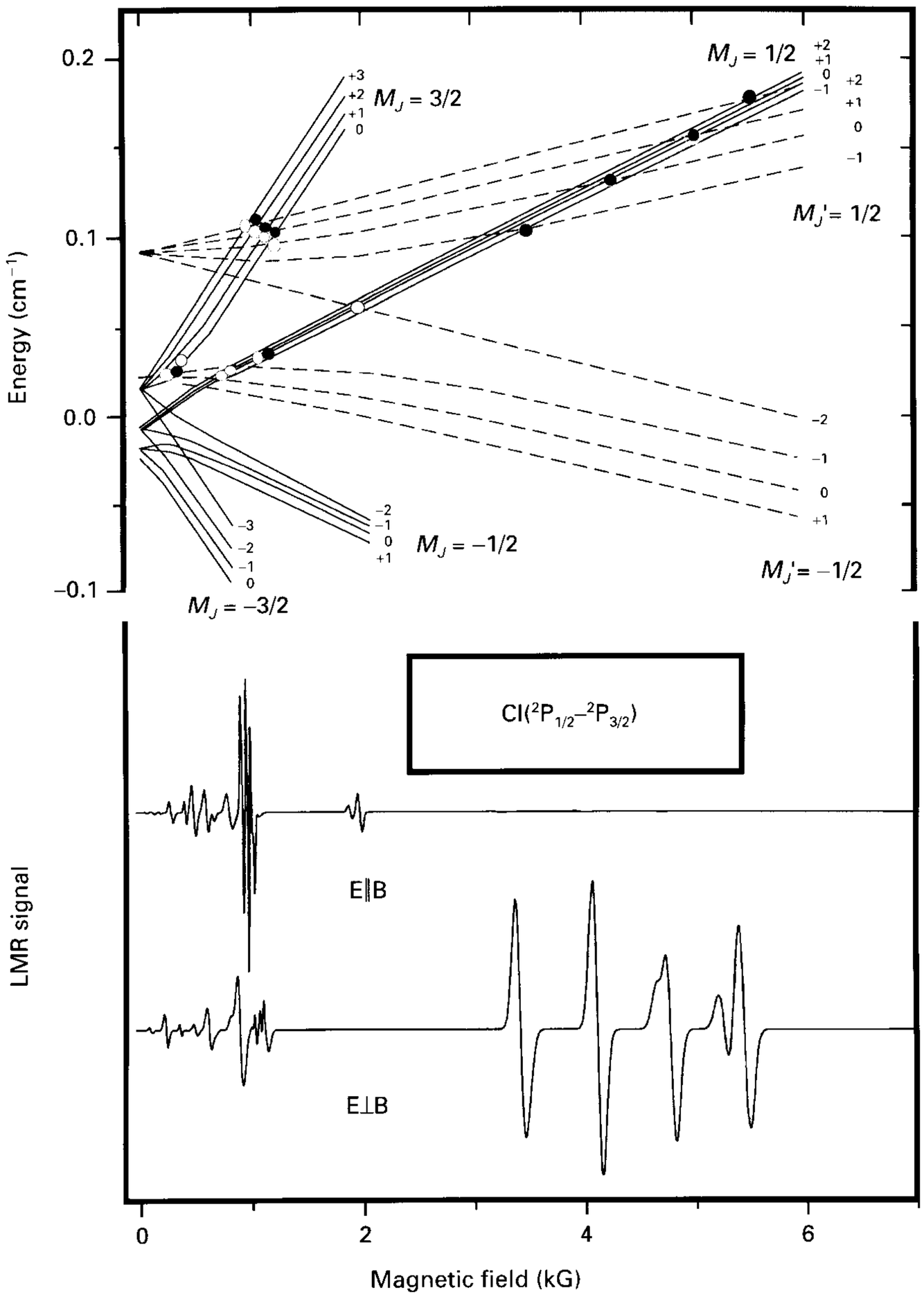

Figure 1 Top: Zeeman effect in ^{35}Cl atoms. All sublevels are labelled by M_F values. The lower $^2P_{3/2}$ state is represented by solid lines. Upper $^2P_{1/2}$ state (dashed lines) is downshifted by an amount of the laser photon energy. Intersections of solid and dashed lines with $\Delta M_F = \pm 1$ (open circles) or with $\Delta M_F = 0$ (solid circles) represent possible LMR transitions. Bottom: LMR spectra of Cl atoms (both ^{35}Cl and ^{37}Cl).

momentum. Centrifugal corrections to some parameters are often used as well as a tensor expression for H_z.

Polyatomic radicals

The most often encountered type of radical observed by LMR is the three-atomic asymmetric-top radical, such as NH_2, PH_2, HCO, HO_2, etc., Hund's case (b). In this case, the Hamiltonian [1] is used. Without spin-orbit and lambda-doubling terms, $H_{\rm rot}$, $H_{\rm ss}$ and $H_{\rm sr}$ are usually expressed as

$$H_{\rm rot} = A_v N_a^2 + B_v N_b^2 + C_v N_c^2 + H_{\rm cd}(\boldsymbol{N}, \Delta_{\rm N}, \Delta_{\rm NK}, \Delta_{\rm K}, \delta_{\rm N}, \delta_{\rm K})$$

$$H_{\rm ss} = \frac{1}{3} D_v (2S_a^2 - S_b^2 - S_c^2) + E_v (S_b^2 - S_c^2)$$

$$H_{\rm sr} = \varepsilon_{aa} N_a S_a + \varepsilon_{bb} N_b S_b + \varepsilon_{cc} N_c S_c$$

where H_{cd} is the Watson's centrifugal distortion operator; the molecule-fixed components of N, S, and ε are labelled by a, b, and c.

Finally note that the representation of the Hamiltonian is very dependent on the particular radical. Some terms are often omitted, and some new ones are added. For example, Jahn–Teller distortion should be taken into account for symmetric top radicals, such as CH_3O and SiH_3.

The LMR detection of polyatomic radicals with heavy (not hydrogen) atoms is hindered for several reasons: (1) the population of the lower state is low, it decreases with rotational partition function; (2) Zeeman splitting is small, it decreases both with moments of inertia and rotational quantum numbers of the radical; hence LMR spectra are observable only at low magnetic fields because of a weak coupling of S with N. Moreover, the spectra are often unresolved because of a large number of components.

An important exception was found for the first time by Uehara and Hakuta who have observed high-field spectra in the ν_1 band of ClO_2 in spite of its small spin-orbit interaction. Later, similar high-field far-infrared LMR spectra of FO_2, ClSO, FSO and NF_2 were detected. These spectra were assigned to transitions induced by avoided crossings between Zeeman levels having the same value of M_J but differing by one in N. This type of transition offers a new means to study radicals which might otherwise be inaccessible to the LMR technique.

LMR spectrometer

Basic features

The essential features of an LMR spectrometer are illustrated schematically in **Figure 2**, which shows three of the most commonly encountered experimental configurations.

A conventional intracavity LMR spectrometer is shown in **Figure 2A**. Placing a free-radical absorption cell inside the laser cavity results in a gain in sensitivity due to multipassing of the laser radiation. A further sensibility gain may also be obtained when the modulation frequency is close to the frequency of the laser intensity relaxation oscillations. Another benefit of the intracavity configuration is that it favours the observation of saturation Lamb dips. This is especially important in the mid-infrared region, where Doppler widths are greater and the high resolution of saturation spectroscopy is needed more. The laser power is coupled out by the zeroth order of the grating and is detected by a photoresistor. Coupling through the hole in one of the mirrors or by a variable coupler inserted into the laser cavity are also used.

An intracavity LMR spectrometer based on an optically pumped laser is shown in **Figure 2B**. The only difference is the change of the CO (or CO_2) laser in **Figure 2A** by an optically pumped laser. The pump radiation is multiply reflected between two metallic-coated flats parallel to the far-infrared laser axis. Longitudinal pumping in which the pump radiation is introduced along the laser axis through a hole in one of the far-infrared laser mirrors is also employed. The cavity is divided by a beam splitter (e.g. thin polypropylene).

Figure 2C gives the block diagram for the Faraday LMR setup, in which there is an extracavity arrangement and detection of paramagnetic species is via their polarization effects. The laser light propagates along the z-axis which coincides with the magnetic field direction. The polarization, determined by the polarizer P_x points along the x-axis and the polarizer P_y points along the y-axis. The multipass absorption cell is placed between these crossed polarizers. The absorbing radicals produce a change in the polarization; this effect is used for sensitive detection of the radicals.

In essence, the Faraday arrangement is extracavity LMR with two crossed polarizers. These polarizers reduce the laser power by a large factor and the LMR signal by the square of that factor. Hence the signal-to-noise ratio for the Faraday arrangement is significantly better (more than two orders of magnitude) than that for conventional extracavity LMR.

Note that time resolution of the intracavity configurations is determined by the medium of the laser: it is usually ~2–4 μs; the time resolution of the Faraday arrangement is considerably better.

The Faraday configuration requires the magnetic field of the electromagnet (solenoid) to be parallel to the Poynting vector, $\boldsymbol{B} \parallel \boldsymbol{S}_p$; An alternative (Voigt) configuration is proposed in which $\boldsymbol{B} \perp \boldsymbol{S}_p$ and a polarization angle relative to $\boldsymbol{B}$ is 45°. Although the Voigt configuration is expected to have similar sensitivity to that of Faraday LMR, it is rarely encountered.

Usually, the configurations in **Figure 2A** and **2C** are used in mid-infrared spectroscopy. The configuration in **Figure 2B** is used in far-infrared spectroscopy only. In intracavity configurations, the polarization of the laser with respect to the magnetic field is determined by the intracavity beam splitter in **Figure 2B** or by windows in **Figure 2A** set at Brewster's angle. The splitter (or the windows) are rotatable about the laser axis so the polarization can be rotated. When the electric vector of the laser lies perpendicular to the magnetic field, $E \perp B$, then

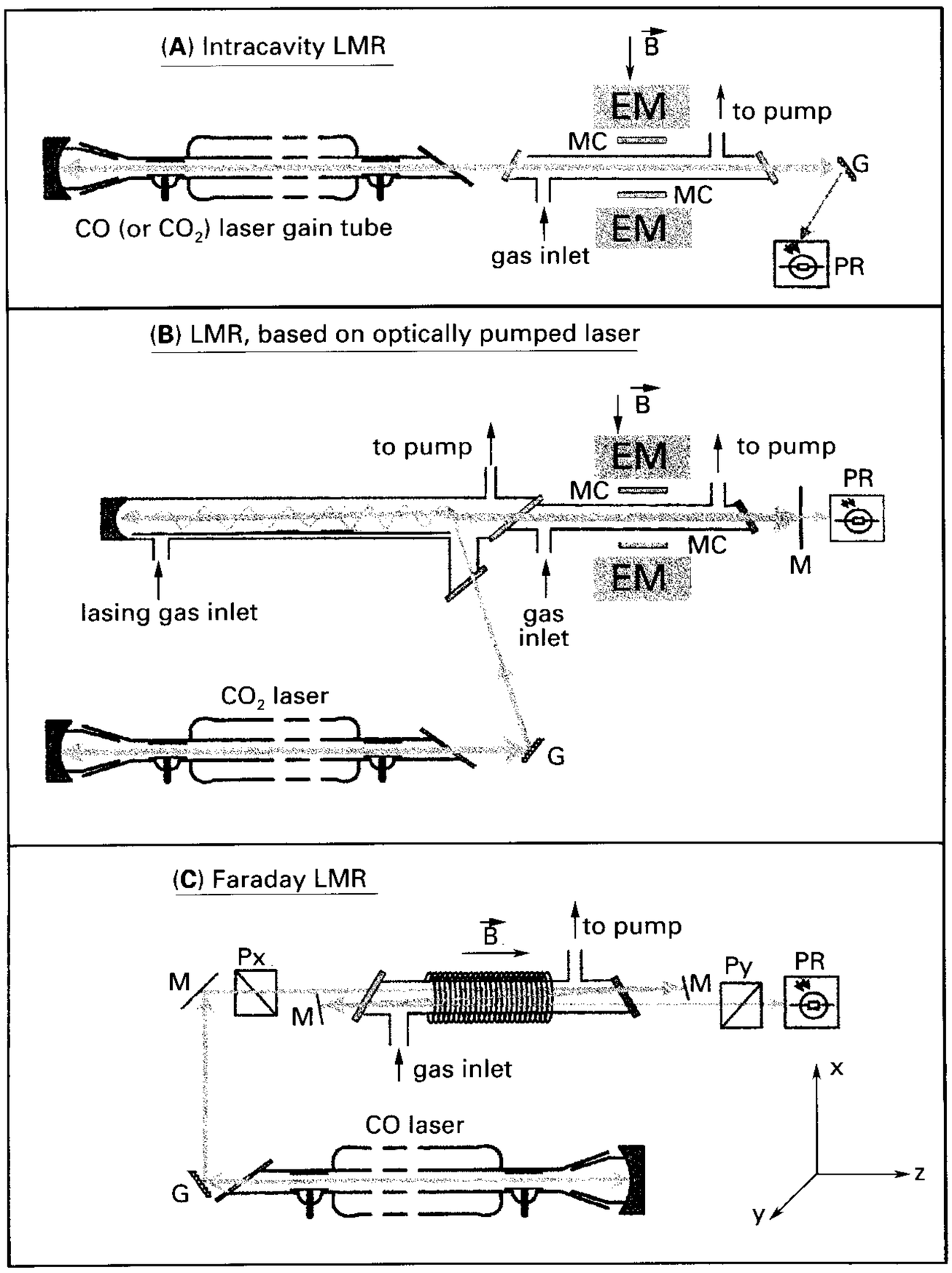

Figure 2 Schematic representation of a LMR spectrometer: (**A**) mid-infrared intracavity arrangement, (**B**) far-infrared intracavity arrangement with optically pumped laser, (**C**) mid-infrared Faraday extracavity arrangement. EM = electromagnet pole, MC = modulation coil, G = diffraction grating, PR = photoresistor, M = mirror, P_x and P_y = polarizers.

$\Delta M_J = \pm 1$ (σ) electric dipole transitions are induced; the $\Delta M_J = 0$ (π) transitions appear with parallel polarization, $E \parallel B$. Note that the latter case is impossible in Faraday LMR.

Infrared lasers

The first far-infrared LMR spectra were recorded by using HCN, H_2O and D_2O lasers. Since then, optically pumped lasers are usually used with a line-tunable continuous-wave CO_2 laser as a light source. By use of these lasers, over 1000 laser frequencies are available in the far-infrared region (30–1200 μm); some 500 have been used in LMR.

In medium-infrared, most of the radical spectra are observed with CO (1200–2000 cm^{-1}) and CO_2 (875–1110 cm^{-1}) lasers. In the former case, the spectral region is now strongly extended by using a CO-overtone laser which provides 200 ($\Delta v = 2$) transitions in the region of 2500–3500 cm^{-1}. In the latter case, a great increase in capacity of LMR (several hundreds of lines) was attained by using $^{13}C^{16}O_2$, $^{13}C^{18}O_2$, $^{13}C^{16}O^{18}O$ and $C^{18}O_2$ isotope modifications; an N_2O laser has also been used.

A colour centre laser (2–4 μm), and spin-flip Raman laser (which consisted of a InSb crystal pumped by a CO laser) have also been employed.

Infrared detectors

The first far-infrared LMR spectra were recorded by using Golay cells. These have the advantage of room temperature operation and are easy to use, but their response is slow and hence only low modulation frequencies (approximately 10–100 Hz) can be used. A further gain in sensitivity was realized by use of a helium-cooled Ge bolometer: the much faster response of the bolometer allows much higher modulation frequencies (~1 kHz), and this, together with the lower noise equivalent power, means that the sensitivity is limited mainly by inherent noise in the laser source. By far the most commonly encountered far-infrared detectors are helium-cooled photoresistors (Ge:B, Ge:In, Ge:Ga, Ge:As, nIn:Sb, etc.); modulation frequencies of up to hundreds of kHz can be used.

In mid-infrared, the most commonly used photoresistors are Ge: Au (77 K), Ge:Hg (53 K), Ge: (Zn, Sb) (64 K) and Hg:Cd:Te (77 K) for CO_2 laser output and Ge:Ga (77 K), In:Sb (77 K), Hg:Cd:Te (77 K) for CO laser output.

In general the main noise source is the laser rather than the photoresistor. However, in the mid-infrared region attenuation of laser light is often required since detectors are easily saturated by laser light. For example, for InSb (77 K) detector saturation starts near 1 mW, while typical CO laser output power reaches 1 W. Note that in Faraday and Voigt LMR arrangements, the saturation is absent.

Modulation

The modulation frequency f is determined as a compromise between two factors. First, at low frequencies the noise of the LMR spectrometer increases due to vibrations of the spectrometer. Second, the modulation amplitude decreases inversely with the square root of f at a fixed power of the generator for modulation coils. Finally, for extracavity LMR the best frequency is 15–20 kHz. For intracavity LMR spectrometers, a gain of sensibility can be obtained when the modulation frequency is close to the frequency of the laser intensity relaxation oscillations (50–150 kHz).

A simple method to improve the sensitivity of LMR is to increase the integration time constant of the lock-in amplifier. However, the long-term instability of the LMR spectrometer usually makes useless time constants larger than 3 s. This problem can be solved by using double modulation. The magnetic field is modulated at high (~100 kHz) and low (~2 Hz) frequencies. The high-frequency signal is demodulated by a phase-sensitive lock-in amplifier. The resulting low-frequency output of the lock-in is again demodulated by another phase-sensitive lock-in. As a result, the effective time constant of the system is ~200 s and the LMR sensitivity increases considerably. Note that the best peak-to-peak amplitude of the low-frequency modulation is equal to the spectral line width. The drawback of this double modulation system is the slow response.

Intracavity systems are very sensitive to acoustic cross talk between the modulation unit and the laser resonator, thus increasing the noise just at the modulation frequency f. Hence another method of improving the sensitivity of intracavity LMR is to use a lock-in detector at $2f$ (the second harmonic), where the noise is considerably smaller. In some cases, this change can increase the signal-to-noise ratio of LMR.

Preparation of radicals

The great majority of radicals studied so far by LMR have been generated by atom–molecule reactions in the gas phase, using discharge-flow techniques or by pumping the products of a microwave discharge rapidly into the sample region of the spectrometer. In addition, a time-resolved arrangement allows generation of radicals either directly by UV photolysis (or multiphoton dissociation), or by the reactions of appropriate molecules with the species prepared photolytically.

Detection of molecular ions

Molecular ions (DCl^+, DBr^+, etc.) are generated by discharge-flow techniques. Two difficulties arise in experiments with intracavity LMR detection of these ions. First is the rapid deflection of the ions to the reactor walls in the magnetic field of the electromagnet; the second is the very high noise of a DC discharge situated inside the laser cavity. These problems have been solved by using the Faraday extracavity LMR arrangement, which does not suffer to the same extent from modulation pickup via discharge plasma as the intracavity arrangement. In the Faraday arrangement the discharge is stable, since the magnetic field of the solenoid and the electric field of the discharge are collinear.

An additional advantage of this arrangement is the possibility of tracing hot-band transitions not only for open-shell ions but also for free radicals.

Sensitivity of LMR, comparison with EPR

The technique of LMR is very similar to other magnetic resonance methods such as EPR and NMR. While NMR uses radiofrequency radiation to produce transitions between nuclear spin levels, and EPR uses microwave radiation to produce transitions between electron spin levels, LMR uses

radiation of a laser to produce transitions between rotational (far-infrared) or vibrational–rotational (mid-infrared) levels in paramagnetic molecules. Note that the sensitivity γ_{min} is nearly equal for EPR and LMR: $\gamma_{min} \simeq 10^{-10}$–$10^{-9}$ cm^{-1}. The concentration sensitivity is given by

$$N_{min} = \frac{\gamma_{min}}{\sigma d}$$

where d is the difference of relative populations of the upper and lower levels and σ is the cross section of the transition. The superiority of LMR over EPR in sensitivity is determined by the d factor (2–3 orders of magnitude) and by the cross section σ which is proportional to the transition frequency. The factor in favour of EPR is the high Q-factor of an EPR resonator. When EPR is compared with mid-infrared LMR, an additional factor in favour of EPR is the dipole transition matrix element, which is an order of magnitude higher for rotational transitions in radicals than that for vibrational–rotational transitions. In general, LMR is much more sensitive than EPR.

The sensitivities of far-infrared intracavity LMR and mid-infrared Faraday LMR are as high as that of laser-induced fluorescence (LIF); the sensitivity of mid-infrared intracavity LMR is usually one order of magnitude less. These estimates, however, are very dependent on the particular radical. The sensitivity achieved in practice also depends on the refinement of the apparatus. The typical values for up-to-date spectrometers are listed in **Table 1**.

For applications in chemical kinetics, combined EPR/LMR spectrometers for both far- and mid-infrared regions have been developed. Three advantages are gained from this arrangement: (i) the versatility of the combined spectrometer, (ii) the possibility of the absolute calibration of the LMR spectrometer by comparison of the LMR and EPR signals of the same radicals, (iii) usage of commercial EPR hardware for LMR detection. In the mid-infrared, EPR and LMR make use of a common detection zone. In the far-infrared, the detection zones of EPR and LMR are placed side by side; they cannot coincide, because of the large wavelength of the far-infrared laser.

Table 1 Typical sensitivities of LMR and EPR

Radical	*Laser*	*Wavelength* (μm)	*Sensitivity* (*cm*$^{-3}$)
Cl	CO_2	11.3	2(9)[a]
O	CH_3OD	145.7	1(10)
Hg	CO	5.67	5(9)
NO	CO	5.33	1(7)
	CH_3OH	1224	1(11)
OH	H_2O	118.6	1(6)
	D_2O	84.3	2(7)
	EPR	30 000	1(10)
O_2	CH_3OH	699.5	5(10)
	EPR	30 000	3(13)
ClO	CD_3I	556.9	2(8)
	H_2O	118.6	4(8)
HO_2	CO_2	10	1(10)
	EPR	30 000	1(13)
NO_2	H_2O	118.6	1(11)
CH_2	$^{13}CH_3OH$	157.9	3(8)
NF_2	CO_2	10	1(10)
	EPR	30 000	1(14)

[a] $a(b) = a \times 10^b$.

In **Table 2** a list of the species detected by LMR to 1998 is presented. However, the pace of developments has slowed, since many of the better-known free radicals accessible for LMR have now been observed. As for lesser-known free radicals, LMR is a difficult method for obtaining initial knowledge (at least for polyatomics) because the Zeeman effect must be analysed as well as the zero-field spectrum. In the mid-infrared, the tunable semiconductor diode lasers are another factor in the development of infrared spectroscopy of high sensitivity and resolution, although LMR provides magnetic parameters inaccessible to the diode laser spectroscopy. In **Figure 3** the rise and the fall of LMR are illustrated.

A typical spectroscopic study of a radical includes: recording of numerous LMR spectra, assignment of the observed resonances to quantum numbers, and determination of the parameters of the Hamiltonian (for both ground and vibrationally excited states in the case of vibrational–rotational spectra). Although the accuracy of these parameters (up to MHz) is somewhat lower than that obtained by microwave spectroscopy, it is not restricted to rotational transitions but includes vibrational, fine structure and hyperfine effects.

The main requirements for a successful LMR study are: (i) the atom or molecule must be paramagnetic ($S > 0$ or $L > 0$); (ii) the closeness of laser and transition frequencies (<1 cm^{-1}); (iii) usually, no more than two heavy (not hydrogen) atoms [exceptions are non-hydride triatomics which are either linear (NCO, N_3, NCN), or which have

Applications of LMR

Spectroscopy studies

LMR has allowed the spectroscopic study of many free radicals that could not be detected by more conventional infrared techniques.

Table 2 Free radicals detected by LMR[a]

H_2O, D_2O, HCN, InSb[b] lasers	OH, OD, CH, O_2, NO, PH, HO_2, NH_2, NO_2, HCO, PH_2
Optically pumped lasers	C, O, Si, CH, CD, CF, O_2, $O^{17}O$, $O^{18}O$, OH, ^{17}OH, OD, NH, ^{15}NH, ND, ClO, SiH, PH, PD, PO, SH, SD, NS, S_2, FeH, CoH, GeH, SeH, SeD, NiH, NiD, CH_2, CD_2, CCH, CH_2F, CH_2Br, CD_2Br, NH_2, NCO, NHD, HO_2, DO_2, FO_2, PH_2, PO_2, ClSO, FSO, FeD_2, CH_3, NH_2O, CH_3O, CH_2OH, N*, Mg*, NF*, O_2*, CO*, CH*, AsH*, CH_2*, OH^+, OD^+, HCl^+, HBr^+
CO_2 laser	Cl, FO, BrO, SH, SD, SO, SiC, NiH, AsO, SeO, NSe, CH_2, $^{13}CH_2$, NH_2, ND_2, PH_2, HO_2, DO_2, HCO, HSO, FCO, FO_2, ClO_2, NO_2, NF_2, SiH_3, SiF_3, CH_3O, Kr*, Xe*, SO*
CO laser	NO, ClO, CD, CF, MgO, SiH, SiD, PH, PD, SD, FeH, CoH, CrH, NiH, NiD, GeH, GeD, AsH, SeH, SeD, SnH, SbH, TeD, C_2H, C_2D, NCN, NCO, NH_2, NO_2, $^{15}NO_2$, N_3, HCO, DCO, HO_2, DO_2, FO_2, FeH_2, Hg*, CO*, NCO*, DCl^+, DBr^+, SD^+

[a] Electronically excited species are marked by *.

[b] Spin-flip Raman laser: InSb crystal pumped by CO laser.

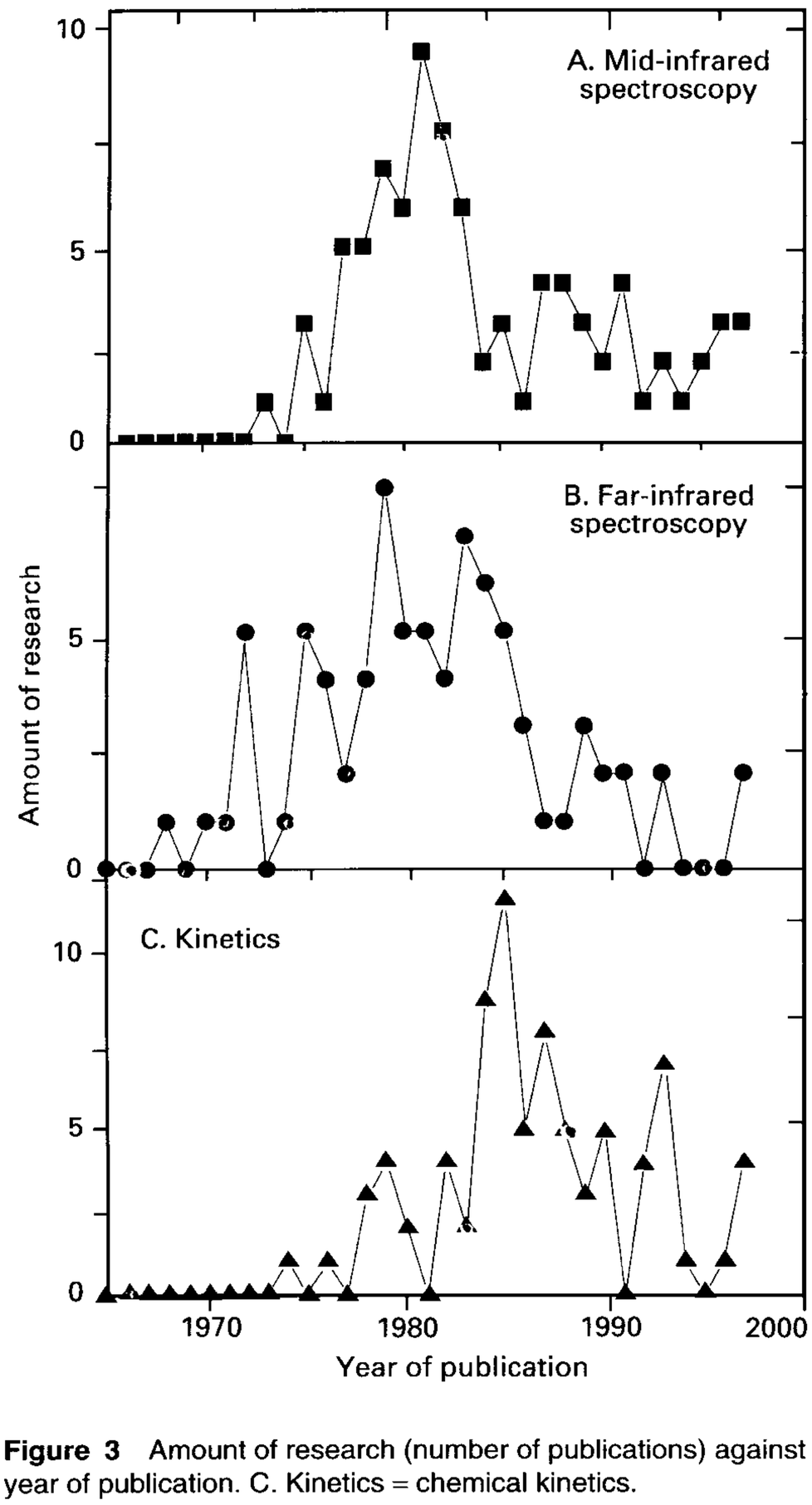

Figure 3 Amount of research (number of publications) against year of publication. C. Kinetics = chemical kinetics.

high-field LMR spectra due to level anticrossing mechanisms (FO_2, ClSO, FSO, ClO_2)]; (iv) a moderate transition dipole moment; (v) numerous resonances at numerous laser lines ought to be detected for successful extraction of the Hamiltonian parameters. If the spectra are complex and energy level predictions are not available, the data from other spectroscopic techniques are especially valid.

LMR in chemical kinetics

The combination of high sensitivity and versatility makes LMR attractive in chemical kinetics studies. Three experimental arrangements of LMR are usually employed.

(i) The first are discharge-flow techniques in which the products of a microwave discharge and consequent chemical reactions are pumped rapidly through the detection zone of a LMR spectrometer. The kinetics are obtained by varying the distance between the radical injector and the detection zone.

(ii) The second is time-resolved LMR in which radicals are produced by either UV photolysis of multiphoton dissociation of a suitable precursor; the LMR signal kinetics is monitored.

These experimental arrangements for kinetics studies are not specific to LMR; they are widely used with other spectroscopic methods, such as EPR, LIF, mass spectrometry, etc.

(iii) The third arrangement is specific to LMR; it is used only to study vibrational relaxation of radicals; an intracavity LMR spectrometer based on a CO_2 laser is usually employed. Radicals are prepared in a discharge-flow system; the kinetics of the LMR signal saturation by a CO_2 laser radiation field after a fast magnetic field jump are monitored. The magnetic field jump provides fast adjustment to the absorption spectral line of the radical. The saturation kinetics are exponential, the exponent decay time being

$$1/\tau = 2\sigma J_0 + \sum_i k_i[\mathrm{M}_i]$$

where σ is the vibrational–rotational transition cross section, J_0 is the photon flux density, $[M_i]$ is the concentration of the ith gas-relaxator and k_i are the vibrational relaxation rate constants. This relation is used to obtain k_i by measuring τ at different $[M_i]$.

This method is applicable only to radicals that show sufficient saturation (>10%) of a vibrational transition by the radiation field. The prerequisites for successful detection of the saturation are: radiation intensity in the cavity of the CO_2 laser of >100 W cm^{-2}, rather a small rotational partition function ($\leq 10^3$, i.e. nonlinear radicals with low moments of inertia, or linear radicals), and moderate transition dipole moment (~0.1 D).

List of symbols

A_{so} = spin-orbit interaction constant; A_v B_v, C_v = rotational constants of radical; a, b = hyperfine constants; $\boldsymbol{B}$ = external magnetic field; d = difference of relative populations; D_v = centrifugal constant for diatomic molecule; D_v, E_v = parameters of Hamiltonian H_{ss}; $\boldsymbol{E}$ = electric field of laser radiation; f = modulation frequency; g_J, g_I = electron and nuclear g-factors; g_s, g_L, g_r = spin, orbital and rotational g-factors; $\hbar$ = Planck's constant; H_{cd} = Watson's centrifugal distortion operator; H_{hfs} = hyperfine interaction operator; H_{ld} = lambda-doubling term in Hamiltonian; H_{rot} = rotational term in Hamiltonian; H_{so} = spin-orbit term in Hamiltonian; H_{sr} = spin-rotational term in Hamiltonian; H_{ss} = spin-spin term in Hamiltonian; H_v = vibrational term in Hamiltonian; H_z = Zeeman term in Hamiltonian; $\boldsymbol{J}$, $\boldsymbol{I}$, $\boldsymbol{F}$, $\boldsymbol{L}$, $\boldsymbol{S}$, $\boldsymbol{N}$, M_F, M_J = momenta and their projections; J_0 = photon flux density; k_i = vibrational relaxation rate constant; $[M_i]$ = concentration of the ith gas-relaxator; N_a, N_b, N_c = components of $\boldsymbol{N}$; N_{min} = concentrational sensitivity; $^2P_{3/2}$, $^2P_{1/2}$ = Cl atomic states; S_a, S_b, S_c, S_z = projections of $\boldsymbol{S}$; S_p = Poynting vector; v = vibrational quantum number; w_e, x_e = parameters of vibrational Hamiltonian; γ = parameter of spin-rotational term H_{sr}; γ_{min} = sensitivity in cm^{-1} units; Δ_N, Δ_{NK}, Δ_K, δ_N, δ_K = centrifugal constants of asymmetric rotor; λ = parameter of spin-spin term H_{ss}; ε_{aa}, ε_{bb}, ε_{cc} = components of spin-rotational tensor; $\mu_0 = e\hbar/2mc$ = Bohr magneton; σ = cross section of the transition; τ = decay time for the saturation kinetics.

See also: **Atomic Absorption, Theory; Electromagnetic Radiation; EPR, Methods; EPR Spectroscopy, Applications in Chemistry; EPR Spectroscopy, Theory; Far-IR Spectroscopy, Applications; High Resolution IR Spectroscopy (Gas Phase) Instrumentation; IR Spectroscopy, Theory; Laser Spectroscopy Theory; Near-IR Spectrometers; Rotational Spectroscopy, Theory; Spectroscopy of Ions; Zeeman and Stark Methods in Spectroscopy, Applications; Zeeman and Stark Methods in Spectroscopy, Instrumentation.**

Further reading

Davies PB (1981) Laser magnetic resonance spectroscopy. *Journal of Physical Chemistry* 85: 2599–2607.

Evenson KM (1981) Far-infrared laser magnetic resonance. *Faraday Discussions of the Chemical Society* 71: 7–14.

Evenson KM, Saykally RJ, Jennings DA, Curl RF and Brown JM (1980) In: Moore CB (ed) *Chemical and Biochemical Applications of Lasers*, Vol 5, p 95. New York: Academic Press.

Hills GW (1984) *Magnetic Resonance Review* 9: 15–64.

Russell DK (1983) *Laser Magnetic Resonance Spectroscopy Electron Spin Resonance: A Specialist Periodical Report the Royal Society of Chemistry*, Vol 8, pp 1–30. London: Royal Society of Chemistry, Burlington House.

Russell DK (1991) *Specialist Periodical Report of the Royal Society of Chemistry* 12B: 64–98.